

respectively. However, in contrast to the preceding cases, the Lifshitz condition is not satisfied and thus one would expect first-order transitions. A LEED study of systems that display these structures would be interesting because observation of a continuous transition would prove the Lifshitz rule violated. Finally, transitions to all  $(a \times a)R\theta$  structures not shown in Fig. 1 are predicted to be first order.

In summary, we have systematically surveyed the transitions to common superlattices on square, triangular, and honeycomb substrates. New results include the prediction of many first-order transitions and continuous transitions in the class of the four-state Potts model. These results have yet to be tested experimentally.

We are extremely grateful to our friends J. G. Dash and S. C. Fain for their enthusiastic support of our work and for acting as our guides through the vast literature on adsorption. We are indebted to David Mukamel for introducing us to Landau theory and for helpful comments. Lastly, we have profited from discussions with R. Alben, R. B. Griffiths, G. Golner, E. K. Riedel, O. E. Vilches, and M. Wortis.

\*Research supported in part by the National Science Foundation under Grants No. DMR73-02582 and No. DMR76-01070.

<sup>1</sup>A recent catalog of such systems is provided by G. A. Somorjai, *Surf. Sci.* **34**, 156 (1973), where experimental observations of most of the structures discussed in this Letter are reported.

<sup>2</sup>A. U. MacRae, *Surf. Sci.* **1**, 319 (1964).

<sup>3</sup>P. J. Estrup, in *The Structure and Chemistry of Solid Surfaces*, edited by G. A. Somorjai (Wiley, New York, 1969), p. 19; S. Andersson, *Nobel Symp.* **24**, 188 (1973).

<sup>4</sup>J. C. Tracy, *J. Chem. Phys.* **56**, 2736 (1972).

<sup>5</sup>M. Bretz and J. G. Dash, *Phys. Rev. Lett.* **27**, 647 (1971).

<sup>6</sup>R. J. Rollefson, *Phys. Rev. Lett.* **29**, 410 (1972);

J. K. Kjems *et al.*, *Phys. Rev. Lett.* **32**, 724 (1974).

<sup>7</sup>M. Bretz, *Phys. Rev. Lett.* **38**, 501 (1977).

<sup>8</sup>S. Alexander, *Phys. Lett.* **54A**, 353 (1975).

<sup>9</sup>R. B. Potts, *Proc. Cambridge Philos. Soc.* **48**, 106 (1952).

<sup>10</sup>S. Krinsky and D. Mukamel, to be published.

<sup>11</sup>L. D. Landau and E. M. Lifshitz, *Statistical Physics* (Pergamon, New York, 1968), 2nd ed. Chap. XIV.

<sup>12</sup>For a detailed account with physical applications see D. Mukamel and S. Krinsky, *Phys. Rev. B* **13**, 5065 (1976).

<sup>13</sup>Thus a classification scheme of two-dimensional transitions based on this rule is invalid; see A. Blandin, *Nobel Symp.* **24**, 194 (1973).

<sup>14</sup>J. P. Straley and M. E. Fisher, *J. Phys. A* **6**, 1310 (1973); R. J. Baxter, *J. Phys. C* **6**, L445 (1973).

<sup>15</sup>D. Mukamel, *Phys. Rev. Lett.* **34**, 481 (1975).

<sup>16</sup>G. Ya. Lyubarskii, *The Application of Group Theory in Physics* (Pergamon, New York, 1960), Chap. VII.

<sup>17</sup>See T. W. Burkhardt *et al.*, *J. Phys. A* **9**, L179 (1976), and references therein.

<sup>18</sup>A first-order transition to this structure was in fact seen in Monte Carlo calculations of K. Binder and D. P. Landau, *Surf. Sci.* **61**, 577 (1976).

<sup>19</sup>R. K. P. Zia and D. J. Wallace, *J. Phys. A* **8**, 1495 (1975).

<sup>20</sup>S. E. Ashley and M. B. Green, *J. Phys. A* **9**, L165 (1976); J. Oitmaa and I. G. Enting, *J. Phys. A* **8**, 1097 (1975).

## Measurement of the Difference between the Dynamic NMR and Static Susceptibilities of Superfluid <sup>3</sup>He-B Using an rf-Biased Superconducting Quantum-Interference Device\*

R. A. Webb

Argonne National Laboratory, Argonne, Illinois 60439  
(Received 24 January 1977)

The temperature-dependent susceptibility of superfluid <sup>3</sup>He-B has been measured both statically and via a pulse technique in a field of 309 G using an rf-biased superconducting quantum-interference device (SQUID). In the pressure range 26.5 to 18 bar, the dynamic NMR susceptibility agrees qualitatively with the theoretical weak-coupling predictions for the Balian-Werthamer state. However, the static susceptibility, measured using the same rf-biased SQUID and detection system, is significantly smaller than the dynamic susceptibility.

The difference between the susceptibility of superfluid <sup>3</sup>He-B as measured statically by superconducting quantum-interference device

(SQUID) techniques and dynamically using NMR techniques is one of the most puzzling experimental discrepancies still existing in superfluid

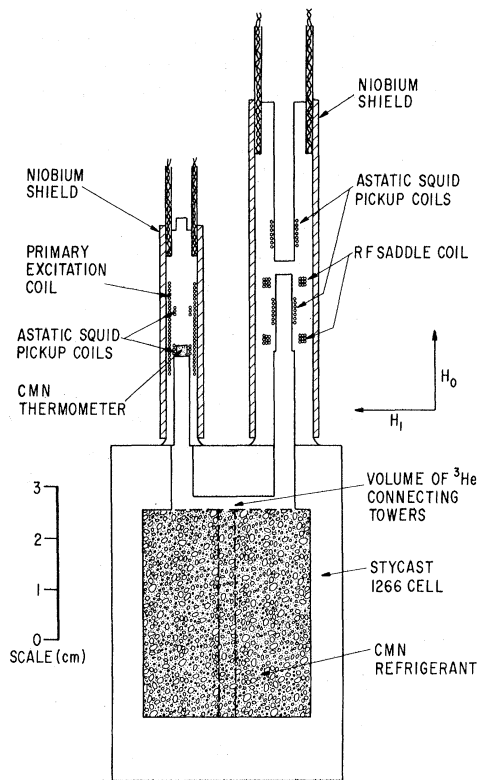


FIG. 1. Schematic drawing of the adiabatic demagnetization cell used in this work.

$^3\text{He}$ . Dynamic NMR measurements, both on and off the melting curve,<sup>1,2</sup> suggest that the temperature-dependent susceptibility of  $^3\text{He-B}$  is qualitatively the same as that predicted by the Balian-Werthamer (BW) theory,<sup>3</sup> while measurements of the static susceptibility using an rf-biased SQUID<sup>4-6</sup> suggest that the susceptibility is significantly smaller than the theoretical predictions. The recent dynamic NMR measurements of Ahoonen *et al.*,<sup>2</sup> made in the same pressure range as the earlier static work, seem to establish that the nature of the resonant magnetism of  $^3\text{He-B}$  is the same both on and off the melting curve. However, the static results have been qualitatively reproduced in at least four different experimental cells employing two different geometries. The main criticism of the static work has been directed toward the procedure used to calibrate the magnetometer, although the value of the diamagnetic susceptibility of  $^3\text{He}$ , a by-product of the calibration, is in reasonable agreement with previous results.<sup>7</sup> The techniques of SQUID NMR have been developed into a usable measuring tool in the millikelvin temperature range and in this work are used to shed new light on this discrep-

ancy. An unambiguous comparison of the dynamic and static magnetism of  $^3\text{He-B}$  has been made by using the same  $^3\text{He}$  sample and detection system. Furthermore, SQUID NMR in the calibration range provides, for the first time, an independent check on the static calibration procedure.

A schematic drawing of the adiabatic demagnetization cell used for the work reported here is shown in Fig. 1. The  $^3\text{He}$  measured was contained in a 3-mm-i.d. tower located above the cerium magnesium nitrate (CMN) refrigerant. The static field  $\vec{H}_0$ , parallel to the axis of the tower, was trapped in a 10.9-mm-i.d. Nb tube. A 42-turn rf saddle coil wound on a diameter of 5 mm with use of 0.076-mm Nb wire provided the transverse field  $\vec{H}_1$ . The  $^3\text{He}$  magnetization was sensed by a 3-mm-long Nb pickup coil wound astatically on a 4.3-mm i.d. The pickup coil was connected to the input coil of a two-hole SQUID operated at 19 MHz in the flux-locked loop configuration.<sup>8</sup> Temperatures were determined from 17-Hz mutual-inductance measurements on 10 mg of CMN located in a second magnetically shielded tower. A provisional absolute temperature scale was obtained by thermally locating the second-order phase transition as a function of pressure and assigning to each magnetic  $T_c^*$  an absolute temperature using the La Jolla diagram.<sup>7</sup>

The calibration of the magnetometer was performed in the conventional way<sup>7</sup> by holding the temperature of the cell constant and allowing liquid to fill the towers slowly while continually monitoring the output of the SQUID. The change in SQUID output is  $\Delta\varphi/\varphi_0 = \lambda(\chi_d + \chi_p)$ , where  $\lambda$  is the calibration constant,  $\varphi_0$  is the flux quantum, and  $\chi_d$  and  $\chi_p$  are the diamagnetic and paramagnetic susceptibilities of  $^3\text{He}$ , respectively. Using the value of  $\chi_p$  determined from measurements of Ramm *et al.*,<sup>9</sup> both  $\chi_d$  and  $\lambda$  were determined from many such cell fills in the temperature range 0.33 to 1.1 K in a static field  $\vec{H}_0$  of 309 G. It was found that  $\chi_d V/n = -(2.08 \pm 0.05) \times 10^{-6} \text{ cm}^3/\text{mole}$  and  $\lambda = (6.38 \pm 0.15) \times 10^7$ . The calibration constant determined statically was checked dynamically in the same temperature range by using both adiabatic fast passage and  $180^\circ$  pulsed NMR. For these two cases the change in SQUID output should be  $\Delta\varphi/\varphi_0 = 2\lambda\chi_p$ . The agreement between the calibration constant determined dynamically and statically was found to be better than  $\pm 2\%$ . Furthermore, at 15 mK in the pressure range 18 to 26.5 bar, the value of  $\lambda$  determined using cw NMR, pulsed NMR, and adiabatic

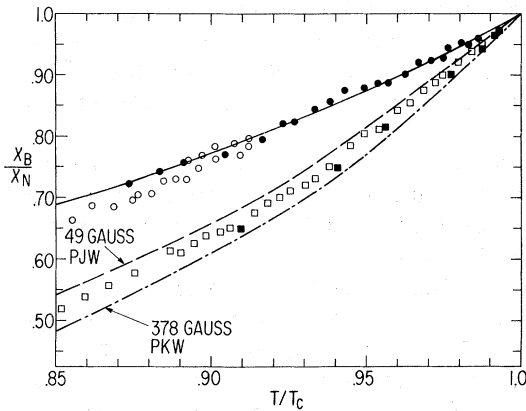


FIG. 2. The normalized susceptibility of  $^3\text{He-B}$  as a function of reduced temperature in a field of 309 G. Open and closed circles are dynamic pulsed SQUID NMR data obtained at a pressure of 26.2 and 18.6 bar, respectively. The solid curve is the theoretical weak-coupling BW susceptibility, assuming  $Z_0 = -3.05$ ; open squares, static susceptibility determined using temperature sweep procedure; closed squares, static susceptibility from  $A-B$  transition; dash-dotted line and dashed line, smoothed static data from Refs. 4 and 5, respectively.

fast passage all agree with the static calibration to  $\pm 1.5\%$ . The details of SQUID NMR as performed in this experiment will be given elsewhere.<sup>10</sup> However, it is important to point out that the main disadvantage of SQUID NMR is that, because of the presence of both the superconducting rf and pickup coils, there is nearly a 3% variation of  $\vec{H}_0$  over our sample region; thus the experimental linewidth tends to be very broad. One of the main advantages of SQUID NMR over conventional NMR is that the change in the component of magnetization parallel to  $\vec{H}_0$  is continuously monitored.

The static susceptibility of superfluid  $^3\text{He-B}$  was determined using two techniques. The first was to measure, as a function of pressure, the size of the jump discontinuity in magnetization upon cooling slowly from the  $A$  phase into the  $B$  phase. This transition was chosen rather than the  $B-A$  because it proved to be "reversible." The second technique was to cool well into the  $B$  phase, establish temperature equilibrium, and then rapidly—within a few seconds—increase the temperature of the main CMN and measure the change in magnetometer output as the  $^3\text{He}$  in the magnetization tower warmed from the initial temperature  $T_i$  through the  $A$  phase into the normal phase. The change in magnetometer output is  $\Delta\phi/\phi_0 = \lambda\Delta\chi_B = \lambda[\chi_N(P) - \chi_B(P, T_i)]$ . Using the

known value of the normal-Fermi-liquid susceptibility and the measured value of  $\Delta\chi_B$ , the value of  $\chi_B(P, T_i)$  can be determined at any temperature. In our field of 309 G the temperature-dependent background magnetization became saturated below  $\sim 4$  mK and thus no background corrections to the static data were necessary. The results of the static susceptibility measurements are shown in Fig. 2 as closed and open squares. The smoothed static data of Paulson, Kojima, and Wheatley<sup>4</sup> in 49 G and of Paulson, Johnson, and Wheatley<sup>5</sup> in 378 G are shown as dashed lines. Our results are in qualitative agreement with the earlier static work and near  $T_c$  are in close agreement with the 49-G data.

The dynamic NMR susceptibility of superfluid  $^3\text{He-B}$  was determined using pulsed SQUID NMR. The data were obtained in the following way: The temperature was held constant by slowly demagnetizing the main CMN, and the recovery of the magnetization of  $^3\text{He-B}$  following an rf pulse was recorded on film. Then by stepping the frequency of the rf pulse off resonance by  $\pm 50$  KHz, the magnitude of the sum of both the background and electronic recovery time could be measured. The SQUID electronic recovery time was determined from independent measurements and found to be 50–100  $\mu\text{sec}$ , depending upon the magnitude of the change in lock point of the flux-locked loop. The background magnetization could usually be separated from the SQUID recovery because of its different time-dependent form. Although the source of the background magnetization is not known, it was found to be fairly reproducible with its magnitude and time for full recovery, being proportional to both the magnitude and direction of the change in the SQUID lock point following the rf pulse. The time for full recovery was generally between 80–180  $\mu\text{sec}$ . The background correction to the on-resonance data, if any, was performed by subtracting an off-resonance background that exhibited the same change of SQUID lock point as the on-resonance data. This correction could be either positive or negative and usually never larger than  $\pm 5\%$  of the total magnetization change of the on-resonance data. For all the work reported here, the width of the rf pulse was held constant at 25  $\mu\text{sec}$  and only its magnitude was varied so as to rotate the spins between  $20^\circ$  and  $100^\circ$ . For these tipping angles we find that the change in  $M_z$  following an rf pulse is proportional to  $1 - \cos\theta$ , where  $\theta$  is the tipping angle. Because of the response time of the flux-locked loop, the initial change in magnetization away

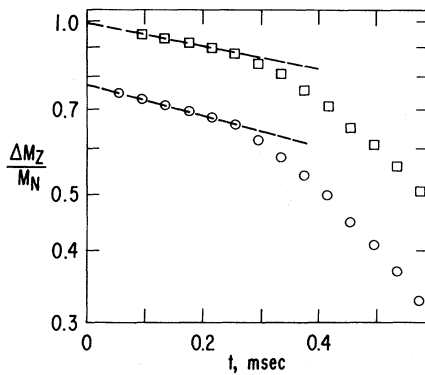


FIG. 3. Initial part of the recovery of the magnetization of both  ${}^3\text{He-A}$  and  ${}^3\text{He-B}$  in a field of 309 G following an rf pulse at a pressure of 26.1 bar. Open circles are  ${}^3\text{He-B}$  data obtained at a  $T/T_c = 0.910$  following a  $92^\circ$  pulse. Open squares are  ${}^3\text{He-A}$  data obtained at  $T/T_c = 0.914$  following a  $62^\circ$  pulse.

from equilibrium following an rf pulse is not observed. Only its recovery toward equilibrium can be measured. To obtain the magnitude of the magnetization, the recovery signal must be extrapolated back to its value at the end of the rf pulse. In Fig. 3 an example of the initial part of the recovery of magnetization following an rf pulse for both  ${}^3\text{He-A}$  and  ${}^3\text{He-B}$  is given at a pressure of 26 bar. The open circles are  ${}^3\text{He-B}$  data obtained after a  $92.4^\circ$  rf pulse at a reduced temperature of  $T/T_c = 0.910$ . For these data there was no change in the lock point of the SQUID following the rf pulse and the data displayed were taken directly from the photographic record with no background corrections made. The dashed line drawn through the first few points is representative of the extrapolation procedure used for all our data although generally the first 80–100  $\mu\text{sec}$  of data can not be used. The recovery of the magnetization after the first 0.5 msec is exponential with a time constant of 0.28 msec. This time constant was nearly temperature and pressure independent, being 0.24 msec at  $T/T_c = 0.84$  and 0.30 msec at  $T/T_c = 0.98$  with a slight dependence on the magnitude of the rf pulse, with  $T_1$  being longer for a larger pulse. The open squares are  ${}^3\text{He-A}$  data obtained at a reduced temperature of  $T/T_c = 0.914$  following a  $62^\circ$  rf pulse. The recovery process for both the *A* and *B* phases appears to be nearly the same. An exponential extrapolation procedure gives a value of  $0.99M_N$  for the *A*-phase susceptibility. For the data displayed in Fig. 3 the recovery of the magnetization after the first 0.7 msec is exponential with

a time constant of 0.33 msec. For all the *A*-phase data far away from  $T_c$  the normal-Fermi-liquid susceptibility is obtained to within  $\pm 2\%$  when using the exponential extrapolation technique. The use of other graphically reasonable extrapolation procedures will systematically lead to a lower value of the  $t=0$  intercept by at most several percent but will not affect the major results of this work.

Representative results of the dynamic data are shown in Fig. 2. The solid curve is the weak-coupling BW theory assuming a value of  $-3.05$  for  $Z_0$  and is seen to describe the 18-bar data well. Although  $Z_0$  is thought to be essentially pressure independent in this pressure range, the 26-bar data may suggest a slight pressure dependence. This result is firmly supported by the earlier dynamic work<sup>2</sup> and seems to indicate that the weak-coupling energy gap is not applicable in this temperature and pressure range. Our 18-bar dynamic data also agree quite well with those of Ref. 2, a result which is quite puzzling in view of the fact that the Helsinki temperature scale is quite different from the La Jolla temperature used in this work. In view of both the temperature-scale question and the possibility of strong-coupling corrections, the agreement of our 18-bar data with a weak-coupling theory may be somewhat fortuitous. Furthermore, the results of Corruccini and Osheroff<sup>1</sup> obtained at melting pressure using the same experimental geometry as employed in this work agree qualitatively with the 29-bar data of Ref. 2, and the temperature scale used for this work<sup>11</sup> is somewhat different than the Helsinki scale.

The measurement of the difference between the dynamic and static susceptibilities of superfluid  ${}^3\text{He}$  as performed in this experiment using the same  ${}^3\text{He}$  sample and detection system, for the first time, strongly suggests that this discrepancy is a real property of the bulk superfluid as yet not understood and can no longer be attributed to an error in the calibration of the magnetometer. This conclusion is independent of temperature-scale questions. Near  $T_c$ , the dynamic data follow  $\chi_B/\chi_N = 1 + 2.6(T - T_c)/T_c$  while the static data can be described by  $\chi_B/\chi_N = 1 + 3.9(T - T_c)/T_c$ .

I wish to acknowledge Mr. Z. Sungaila for his assistance in data acquisition during part of this experiment. I gratefully acknowledge many useful conversations with Dr. Pat Roach, Dr. Paul Roach, Professor J. B. Ketterson, and Professor J. C. Wheatley.

\*Work supported by the U. S. Energy Research and Development Administration.

<sup>1</sup>L. R. Corruccini and D. D. Osheroff, Phys. Rev. Lett. **34**, 695 (1975).

<sup>2</sup>A. I. Ahonen, T. A. Alvesalo, M. T. Haikala, M. Krusius, and M. A. Paalanen, Phys. Lett. **51A**, 279 (1975); and A. I. Ahonen, M. Krusius, and M. A. Paalanen, J. Low Temp. Phys. **25**, 421 (1976).

<sup>3</sup>A. J. Leggett, Rev. Mod. Phys. **47**, 331 (1975).

<sup>4</sup>D. N. Paulson, H. Kojima, and J. C. Wheatley, Phys. Rev. Lett. **32**, 1098 (1974).

<sup>5</sup>D. N. Paulson, R. T. Johnson, and J. C. Wheatley,

Phys. Rev. Lett. **31**, 746 (1973).

<sup>6</sup>R. A. Webb, R. E. Sager, and J. C. Wheatley, J. Low Temp. Phys. **26**, 439 (1977).

<sup>7</sup>J. C. Wheatley, Rev. Mod. Phys. **47**, 415 (1975).

<sup>8</sup>R. P. Giffard, R. A. Webb, and J. C. Wheatley, J. Low Temp. Phys. **6**, 533 (1971).

<sup>9</sup>H. P. Ramm, P. Pedroni, J. R. Thompson, and H. Meyer, J. Low Temp. Phys. **2**, 539 (1970).

<sup>10</sup>R. A. Webb, to be published.

<sup>11</sup>W. P. Halperin, C. N. Archie, F. B. Rasmussen, R. A. Buhrman, and R. C. Richardson, Phys. Rev. Lett. **32**, 927 (1974).

## Rare-Earth Ultrasonic Attenuation in Applied Fields

D. T. Vigen

*Institut für Theoretische Physik, Freie Universität—Berlin, Berlin, West Germany*

(Received 27 December 1976; revised manuscript received 14 February 1977)

I show that dynamic screening of phonons by spin-polarized conduction electrons is an important mechanism for anomalous field-dependent acoustical absorption in heavy rare-earth metals. The absorption coefficient is larger by a factor  $\{\partial[N(E_F)]^{-1}/\partial E\}^2$  than that arising from the presently accepted mechanism of exchange modulation. Here  $N(E_F)$  is the density of states at the Fermi energy. The expected behavior in degenerate magnetic semiconductors is also discussed and interesting predictions for experiment are made.

Acoustical absorption in the paramagnetic region of heavy rare-earth metals increases as  $H^2$  in low fields.<sup>1,2</sup> This is in contrast to the expectations of the conventional theory<sup>3</sup> in which phonons scatter from spin fluctuations, since these fluctuations are suppressed by the applied field. Tachiki and Maekawa<sup>4</sup> recognized the importance of off-resonance response of the local  $4f$  spins to sound vibrations, and proposed that absorption arises through phonon modulation of the indirect-exchange interaction (volume magnetostriction). Recently, Kim<sup>5</sup> has demonstrated the importance of screening by conduction electrons, in explaining anomalous, *zero-field* absorption in the paramagnetic phase of itinerant magnets. In these materials the electron-density response is strongly exchange-enhanced, increasing sharply as the Curie temperature,  $T_C$ , is approached from above. Electron density polarization, coupled to the lattice motion through the electron-phonon interaction, becomes easier as a result of exchange enhancement, so that a softening of the longitudinal phonons and enhanced sound attenuation are predicted.

In rare-earth metals, exchange enhancement among the  $5d$ - $6s$  conduction electrons is much weaker and itinerant magnetism is not observed. There is no dramatic increase in the electronic

response near  $T_C$ , below which the well-localized  $4f$  moments order magnetically, and in zero field I do not expect anomalous attenuation from a dynamical screening mechanism. A magnetic field, however, induces long-range order among the  $4f$  spins, and the conduction spin sub-bands split in the strong  $c$ - $f$  (i.e.,  $s$ - $f$  or  $d$ - $f$ ) exchange field. Repopulation in the spin sub-bands produces a spin polarization in the electronic density at the Fermi surface.

In this Letter I show that dynamic screening of phonons by spin-polarized conduction electrons is an important mechanism for explaining anomalous field-dependent absorption in the rare-earth metals: The spin-polarized electrons move to screen the electric perturbation and induce an energy-dissipating off-resonance response among the  $4f$  electrons, via the  $c$ - $f$  exchange interaction. The effect becomes especially important near  $T_C$ , where the magnetic response of the  $4f$  moments becomes large.

The ionic charge-density oscillations, created by a longitudinal ultrasonic wave of amplitude  $u_0$ , wave vector  $\vec{q}$ , and frequency  $\Omega$ , that is propagating along the  $c$  axis ( $z$  direction) of an hcp metal may be written as

$$\delta\rho(\vec{r}, t) = -iz_0en_0u_0qe^{i(qz - \Omega t)},$$